DOE/NASA/1044-79/4
NASA TM-79252

PERFORMANCE OF A 22.4-kW NONLAMINATED-FRAME dc SERIES MOTOR WITH CHOPPER CONTROLLER

John R. Schwab
National Aeronautics and Space Administration
Lewis Research Center

September 1979

Prepared for
U.S. DEPARTMENT OF ENERGY
Conservation and Solar Applications
Transportation Energy Conservation Division

NOTICE

DOE/NASA/1044-79/4
NASA TM-79252

PERFORMANCE OF A 22.4-kW NONLAMINATED-FRAME dc SERIES MOTOR WITH CHOPPER CONTROLLER

John R. Schwab
National Aeronautics and Space Administration
Lewis Research Center
Cleveland, Ohio 44135

September 1979

Work performed for
U.S. DEPARTMENT OF ENERGY
Conservation and Solar Applications
Transportation Energy Conservation Division
Washington, D.C. 20545
Under Interagency Agreement EC-77-A-31-1044

SUMMARY

Very little performance data is available for chopper controlled dc series motors as used in battery powered electric vehicles. This report presents performance data obtained through experimental testing of a 22.4 kW (30 hp) traction motor using two types of excitation: ripple-free dc from a motor-generator set for baseline data and pulse-width modulated (chopped) dc as supplied by a battery and chopper controller. For the same average values of input voltage and current, the power output was independent of the type of excitation. However, at the same speeds, the motor efficiency at low power output (corresponding to low duty cycle of the controller) was 5 to 10 percentage points less on chopped dc than on ripple-free dc. This apparent discrepancy illustrates that for chopped dc waveforms, it is incorrect to calculate input power as the product of average voltage and current. The chopped dc locked-rotor torque was approximately 1 to 3 percent greater than the ripple-free dc locked-rotor torque for the same average values of current.

INTRODUCTION

Direct-current series motors with chopper controllers are used in the majority of present-day batter powered electric vehicles (ref. 1). The chopper controller is a dc to dc converter that produces a variable average output voltage from a reasonably constant voltage source. Very little performance data is available for dc motors operating under the pulse modulation voltage control provided by such controllers. Many electric vehicle manufacturers are small companies with limited capacity for testing, research and development of propulsion system components. They are usually forced to choose a traction motor based only upon the limited data provided by the motor manufacturer for ripple-free dc operation.

E-163

The NASA Lewis Research Center has been given responsibility by the Department of Energy to conduct research, development, and testing of propulsion systems and components for electric and hybrid vehicles. Part of the Lewis Research Center program is focused upon characterizing existing propulsion system components. The data presented in this report is a result of the characterization effort and will assist present-day electric vehicle manufacturers. The data will also support the development of improved components by providing a comparison baseline.

The motor that was tested and the controller have both been used in electric vehicles, although no known vehicle has used them in combination. The motor was experimentally tested under a wide range of operating conditions for two types of excitation: ripple-free dc as supplied by a motor-generator set for baseline motor data, and chopped dc as supplied by the chopper controller and battery pack. Motor efficiency and motor output power were calculated for comparison of motor performance under both types of excitation. The locked-rotor torque was also determined.

DESCRIPTION OF MOTOR AND CONTROLLER

The motor for which performance data is presented in this report was manufactured by Avon Manufacturing, Inc. of Avon Lake, Ohio, and is shown mounted on the test stand in figure 1. It is electrically similar to the Baker motor used in the Otis P500 electric van. The motor is a four-pole series field machine with a wave wound armature and an 81-bar commutator. Although the frame is nonlaminated, the poles are constructed from die-cut laminations and bolted to the frame. Forced ventilation is required for the maximum continuous rated output power of 22.4 kW (30 hp). Additional rating data and dimensions are given in table I. The brushes were shifted approximately 30 electrical degrees clockwise (cw) off the geometric neutral position by the manufacturer. This brush shift makes counterclockwise (ccw) rotation the preferred direction of rotation for the motor.

The controller was manufactured by EVC, Inc., of Inglewood, California, using high current power Darlington switching transistors produced by the Semiconductor Division of EVC, Inc. Voltage control is accomplished by pulse width modulation from 0 to 100 percent duty cycle at a nominal switching rate of 400 Hz. Since duty cycle variations caused the switching rate to deviate somewhat from the nominal value, a minor modification of the controller was made at NASA to keep the switching rate constant. This change eliminated any of the effects of variable switching rate from the test results. A frequency counter was used to monitor the switching rate during the tests. The controller contains an internal flywheel diode and an input capacitor filter along with current limit, short circuit, and thermal limit protection circuits. Rating data and dimensions are given in table II. A photograph of the controller is shown in figure 2.

APPARATUS AND PROCEDURE

A block diagram of the apparatus used in the motor testing is shown in figure 3. The drive motor was used for the no-load loss tests. An electrical connection diagram for the chopper controlled motor tests is shown in figure 4. To eliminate erratic controller operation due to battery voltage droop at high current levels, a separate 12 V dc power supply was used to power the controller logic circuits.

Maximum values of the measurands recorded, along with their estimated accuracies, are listed in table III. A block diagram of the instrumentation system is shown in figure 5. Coaxial shunts with extended frequency response, negligible phase shift, and very large energy capacity were used for current measurements. Wideband electronic wattmeters were used to measure electrical power. Reference 2 discusses the attributes of such instrumentation.

The motor wattmeter was used to measure the average electrical input power to the motor for both the ripple-free dc tests and the chopped dc tests in order to maintain consistent power measurements and to allow valid efficiency comparisons. Static and dynamic calibrations were performed on the wattmeter to check its accuracy.

Figure 6 shows the relationship of indicated power to calculated power for the static ripple-free dc calibration. Signal generators were used to provide appropriate voltage and current signals. The calculated power was computed as the product of voltage and current signals. Figure 7 presents the correlation of indicated power to calculated power for the static chopped waveform calibration. For this test, the inputs consisted of 500 Hz rectangular pulse trains supplied by synchronized signal generators. The pulse train amplitudes were set equal to the full scale dc voltage and current signals. The calculated power was computed as the product of the voltage amplitude, current amplitude, and duty cycle. The straight line plotted on each graph represents the perfect theoretical correlation; the actual data points correspond within ±2 percent of full scale.

The results of the dynamic calibration are presented in figure 8. For this test, the wattmeter inputs consisted of actual voltage and current signals during ripple-free dc operation of the motor. The calculated power was computed as the product of the average voltage and the average current. The data points lie within ±600 W of the perfect theoretical correlation line; this accuracy corresponds to ±2 percent of the 30 kW maximum power.

The scanning data logger with averaging input was used to record all measurands except temperature, which was visually monitored during the tests. The amplifiers in the instrumentation system were wideband, floating differential input types used to provide good isolation from the power circuits and high common-mode signal rejection. Oscilloscope trace photographs of the instantaneous voltage and current signals were taken at various data points.

Baseline motor performance was established by a series of ripple-free dc motor tests, powered by a large dc motor-generator set. For the chopper controlled motor tests, an 84 V battery pack consisting of 14 EV-106 lead batteries was used. The battery pack was recharged whenever the open-circuit terminal voltage dropped below 80 V, which is approximately 95 percent of the 84 V nominal value. This procedure minimized the effects of battery state of charge on the test results.

The motor temperature was monitored by a thermocouple on one of the motor field coils. This temperature was maintained between 70° and 80° C for all motor performance tests by varying the warm-up loading and the cooling ventilation of the motor. An average winding temperature of 75° C was assumed for all winding resistance calculations.

The cw brush shift made the preferred direction of rotation ccw; all tests were performed with ccw rotation. The mechanical losses tests were run at various speeds and various average field current levels. The motor performance tests were run by varying the average motor voltage and motor speed to obtain several parametric matrices of data points.

RESULTS AND DISCUSSION

The motor performance data is presented in tables IV, V, and VI. In table IV the independent variables are average voltage and average current. In table V the independent variables are average voltage and speed. In table VI the independent variables are average current and speed. Speed and torque were measured and motor output power was calculated in English units and then converted into SI units for the tables. The motor input power was measured by the electronic wattmeter. Figure 9 shows the output power of the motor as a function of speed, average voltage, and average current for ripple-free dc and chopped dc. The power developed by the motor at any particular speed, average voltage, and average current is virtually the same for either type of excitation. Since the controller went into continuous conduction (100 percent duty cycle) above the 70 V level, 80 V and 100 V data could not be obtained when operating with the EVC controller and the 84 V battery pack. During continuous conduction, the battery pack could not maintain 80 V at any of the current levels. Efficiency was calculated as the ratio of output power as determined from speed and torque to input power as measured by the wattmeter. Figure 10 presents motor efficiency as a function of output power and speed. The difference in efficiency appears to be 5 to 10 percentage points less when the motor is operated with the chopper controller at the lower power levels (corresponding to low controller duty cycles). As the power level and the average applied voltage increase, the difference between the chopped dc efficiency and the ripple-free dc efficiency becomes smaller. The efficiency curves meet when the controller duty cycle is close to 100 percent. The estimated error in the efficiency data is ±3 percent.

The lower chopped dc efficiency suggests additional electrical or magnetic loss mechanisms in the motor during chopped dc operation, especially at low average voltage levels when the crest factor (peak to average ratio) of the applied waveform is very high. Since the output power is the same for identical combinations of speed, average voltage, and average current for both types of excitation, this also illustrates that for chopped waveforms, which contain an appreciable ac component, it is incorrect to calculate the motor input power as the product of average voltage and average current. Some possible loss mechanisms that may occur during chopped dc operation of the motor are:

1. Increased effective impedance due to nonuniform current distribution (skin effect and proximity effect) caused by the ac components of the current.

2. Additional I^2R losses at the same average current level due to the rms value of the ac components of the current.

3. Increased commutation losses caused by higher induced voltages in short-circuited armature windings undergoing commutation.

4. Increased brush voltage drop due to ac components in the armature current.

5. Poor commutation due to ac components in the armature current.

6. Eddy-current and hysteresis losses in the stator frame and poles due to the chopped current waveform.

7. Increased direct-axis flux distortion under load due to armature reaction magnetomotive force created by the chopped armature current waveform.

8. Additional magnetic reluctance and airgap flux distortion due to varying permeability of magnetic circuit (especially the pole faces) under varying flux conditions.

Some typical chopped dc motor voltage and current waveforms are shown in figure 11. Because of the action of the flywheel diode in the controller, the current waveforms exhibit different time constants for build-up and decay. The reason for the different time constants is that during build-up, the battery resistance is present in the circuit, while during decay, only the motor resistance and low flywheel circuit impedance are present.

Locked-rotor torque data is tabulated in table VII and presented graphically in figure 12. The chopped dc torque is greater than the ripple-free dc torque for the same average current. Since the brushes are shifted in the motor, a possible explanation is that the ac component of the chopped current in the series field induces voltages in the armature which cause additional currents to flow when the brushes are not located on the neutral position. This effect would be similar to the operation of an ac repulsion motor.

The mechanical losses data is presented in figure 13. The brush friction curve has a power curve fit exponential of 0.993 compared to 1.873 for the bearing friction and windage curve. Brush friction is clearly the predominant mechanical loss mechanism.

The I^2R losses data is presented in figure 14. These losses consist of resistive joule heating losses in the armature windings, series field windings, and brushes. The voltage drop of the brushes is reasonably approximated as 1.0 V at 50 A, 1.2 V at 100 A, 1.4 V at 150 A, 1.6 V at 200 A, 1.9 V at 250 A, and 2.3 V at 300 A. The measured armature and field windings resistances were adjusted for the assumed constant winding temperature of 75^{o} C. For the ripple-free dc excitation, the average and rms values of the current are the same and the average value may be used to determine the I^2R loss. For the chopped dc excitation, the rms value of the current will be greater than the average value due to the ac component, and the joule heating losses will be greater. For either type of excitation, the I^2R losses constitute the principle loss mechanism in this relatively high current, low voltage motor.

SUMMARY OF RESULTS

The Avon motor was tested to determine its performance when operated with the EVC chopper controller and a battery pack. Baseline ripple-free dc performance data was obtained by exciting the motor from a variable-voltage motor-generator set. Locked-rotor torque and mechanical losses were also determined.

The difference in efficiency appears to be 5 to 10 percentage points less when the motor is operated with the chopper controller at low output power levels. At higher output power levels, as the controller duty cycle approached 100 percent, the chopped dc efficiency approached the ripple-free dc efficiency. The output power developed for the same average voltage and average current was virtually identical for both types of excitation. The chopped dc locked-rotor torque was approximately 1 to 3 percent greater than the ripple-free dc torque for the same average values of current.

REFERENCES

1. State-of-the Art Assessment of Electric and Hybrid Vehicles. CONS/1011-1, NASA TM-73756, 1977.

2. Triner, James E.; and Hansen, Irving G.: Electric Vehicle Power Train Instrumentation - Some Constraints and Considerations. ERDA/NASA - 1011/77/1, NASA TM X-73629, 1977.

TABLE I. - MOTOR DATA

Manufacturer	Avon Manufacturing, Inc.
Model number	107971A
Serial number	75281
Rated continuous output power, kW (hp)	22.4 (30)
Rated dc voltage, V	96
Rated dc current, A	300
Rated speed, rad/s (rpm)	419 (4000)
Insulation class	H
Overall frame diameter, m (in.)	0.30 (11.8)
Overall frame length, m (in.)	0.39 (15.3)
Mass, kg (lbm)	91 (200)
Armature resistance at 25° C, ohms	0.011
Field resistance at 25° C, ohms	0.005
Brush shift, electrical degrees	30° cw
Preferred direction of rotation, viewed from anti-drive end	ccw

TABLE II. - CONTROLLER DATA

Manufacturer	EVC, Inc.
Model number	400-96-12-H
Serial number	1405
Maximum input voltage, V	96
Maximum output current, A	400
Overall length, m (in.)	0.26 (10.3)
Overall width, m (in.)	0.18 (7.3)
Overall depth, m (in.)	0.10 (4.0)
Mass, kg (lbm)	5.7 (12.5)

TABLE III. - MEASURANDS AND ACCURACIES

Measurand	Full-scale calibration	Accuracy, percent full-scale
Average input voltage	100 V	±0.5
Average input current	300 A	±0.5
Average input power	30.0 kW	±2.0
Average motor voltage	100 V	±0.5
Average motor current	300 A	±0.5
Average motor power	30.0 kW	±2.0
Motor speed	524 rad/s (5000 rpm)	±0.2
Motor torque	108.5 N-m (80.0 lbf-ft)	±0.5
Motor temperature	100° C	±2.0

TABLE IV. - MOTOR PERFORMANCE DATA WITH AVERAGE VOLTAGE AND AVERAGE CURRENT AS INDEPENDENT VARIABLES

(a) Ripple-free dc

Average voltage, V	Average current, A	Motor input power, W	Torque, N-m	Speed, rad/s	Motor output power, W	Efficiency, percent
9.9	52.9	763	1.8	88	155	20.3
9.8	102.5	1 308	12.9	38	491	37.5
19.9	52.9	1 191	1.8	207	364	30.6
20.0	102.5	2 243	12.9	106	1 368	60.9
20.0	152.3	3 255	30.2	70	2 106	64.7
19.7	202.0	4 307	50.9	51	2 583	59.9
40.1	102.6	4 151	13.3	233	3 087	74.4
40.5	153.9	6 333	30.2	164	4 956	78.3
40.2	203.6	8 319	51.9	126	6 532	78.5
40.4	253.3	10 422	77.3	104	8 013	76.9
40.2	303.0	12 526	106.2	88	9 306	74.3
60.3	104.2	6 021	12.6	353	4 436	73.7
59.8	153.9	9 137	30.9	247	7 602	83.2
60.0	201.9	12 214	53.3	194	10 296	84.3
60.5	253.3	15 564	79.7	162	12 892	82.8
60.3	303.0	18 563	107.8	140	15 116	81.4
80.0	152.3	11 980	30.5	335	10 195	85.1
80.3	203.6	16 265	53.9	262	14 101	86.7
80.4	251.7	20 471	79.7	220	17 492	85.4
80.3	303.0	24 600	108.9	191	20 730	84.2
100.0	203.6	20 316	53.3	329	17 467	86.0
99.9	253.3	25 456	80.0	275	21 917	86.1
100.2	303.0	30 871	109.6	241	26 286	85.1

(b) Chopped dc (400 Hz)

Average voltage, V	Average current, A	Motor input power, W	Torque, N-m	Speed, rad/s	Motor output power, W	Efficiency, percent
10.1	52.9	996	2.0	97	197	19.8
9.9	101.0	1 697	11.9	45	537	31.6
19.9	52.9	1 581	2.7	206	557	35.2
20.1	99.4	2 671	12.6	117	1 467	54.9
20.1	153.9	3 801	29.8	75	2 218	58.4
20.2	202.0	4 697	52.6	53	2 804	59.7
20.2	250.0	5 670	77.0	41	3 178	56.0
39.9	54.5	2 593	3.4	399	1 349	52.0
39.9	100.9	4 463	14.2	233	3 307	74.1
39.4	147.5	6 177	29.2	165	4 805	77.8
39.9	200.4	8 825	51.9	127	6 581	74.6
39.9	253.3	10 890	79.3	102	8 058	74.0
40.2	301.4	12 837	107.5	87	9 358	73.0
59.9	104.2	6 371	13.6	356	4 821	75.7
60.2	152.3	9 215	29.2	258	7 498	81.4
59.7	200.4	12 253	51.9	196	10 132	82.7

TABLE V. - MOTOR PERFORMANCE DATA WITH AVERAGE VOLTAGE AND SPEED AS INDEPENDENT VARIABLES

(a) Ripple-free dc

Average voltage, V	Average current, A	Motor input power, W	Torque, N-m	Speed, rad/s	Motor output power, W	Efficiency, percent
10.0	84.9	1 074	8.8	53	467	43.5
19.8	197.2	4 034	48.8	53	2 556	63.4
9.9	51.3	724	1.8	105	184	25.4
20.1	107.4	2 204	14.9	105	1 565	71.0
40.2	246.9	9 916	74.6	105	7 826	78.9
20.4	56.1	1 191	2.4	210	512	42.9
39.9	113.8	4 424	17.4	210	3 639	82.3
60.3	185.9	10 929	45.2	210	9 481	86.8
80.2	266.1	21 250	87.2	210	18 279	86.0
39.9	76.9	2 865	5.8	315	1 832	63.9
60.0	118.6	6 800	17.6	315	5 545	81.5
80.0	165.1	12 954	35.7	315	11 208	86.5
99.7	218.0	21 445	59.4	315	18 665	87.0
40.0	56.1	2 009	2.4	420	1 022	51.1
60.2	86.6	4 775	8.8	420	3 692	77.3
80.1	117.0	8 903	18.0	420	7 560	84.9
100.5	153.9	14 940	30.9	420	12 960	86.7

(b) Chopped dc (400 Hz)

Average voltage, V	Average current, A	Motor input power, W	Torque, N-m	Speed, rad/s	Motor output power, W	Efficiency, percent
9.8	86.5	1 425	8.5	54	458	32.1
20.0	203.6	4 697	51.9	53	2 719	57.9
9.8	46.5	918	1.4	106	143	15.6
20.1	110.6	2 905	14.9	105	1 560	53.7
40.3	250.0	10 695	77.0	105	8 033	75.1
19.9	52.9	1 542	2.4	210	512	33.2
39.7	117.0	5 203	17.6	211	3 701	71.1
59.4	184.3	11 045	43.8	211	9 196	83.3
39.9	73.7	3 606	6.5	315	2 043	56.7
59.8	118.6	7 306	18.0	315	5 662	77.5
38.9	51.3	2 593	1.8	419	737	28.4
59.8	84.9	5 242	8.1	421	3 413	65.1

TABLE VI. - MOTOR PERFORMANCE DATA WITH AVERAGE CURRENT AND SPEED AS INDEPENDENT VARIABLES

(a) Ripple-free dc

Average voltage, V	Average current, A	Motor input power, W	Torque, N-m	Speed, rad/s	Motor output power, W	Efficiency, percent
6.5	52.9	646	2.4	53	129	19.9
11.7	102.6	1 386	13.6	53	710	51.2
16.3	153.9	2 671	30.5	53	1 598	59.8
20.3	203.6	4 268	51.5	53	2 714	63.6
24.1	253.3	6 255	75.9	53	4 000	63.9
27.7	303.0	8 514	104.4	53	5 522	64.9
10.5	52.9	762	2.0	105	213	27.9
19.4	102.6	2 087	13.6	105	1 423	68.2
27.4	153.9	4 190	30.5	105	3 201	76.4
34.5	202.0	6 995	52.2	105	5 478	78.3
41.2	253.3	10 422	77.9	105	8 181	78.5
46.9	303.0	14 278	106.5	105	11 169	78.2
19.5	52.9	1 074	2.0	210	426	39.7
36.7	104.2	3 684	13.9	210	2 928	79.5
51.1	152.3	7 579	30.5	211	6 406	84.5
64.9	203.6	13 032	53.9	210	11 293	86.7
77.2	253.3	19 459	80.0	210	16 773	86.2
87.7	303.0	26 664	109.2	210	22 885	85.8
28.5	52.9	1 503	1.4	315	426	28.3
52.7	102.6	5 125	12.6	315	3 967	77.4
74.6	153.9	11 007	30.2	315	9 503	86.3
94.7	203.6	19 030	52.9	315	16 636	87.4
38.3	52.9	1 853	2.0	420	852	45.9
71.2	102.6	6 839	13.3	420	5 562	81.3
100.5	153.9	14 940	30.9	420	12 960	86.7

(b) Chopped dc (400 Hz)

Average voltage, V	Average current, A	Motor input power, W	Torque, N-m	Speed, rad/s	Motor output power, W	Efficiency, percent
6.3	51.3	762	1.8	53	93	12.2
11.2	100.9	1 775	11.5	54	621	35.0
15.8	155.5	3 061	30.2	53	1 583	51.7
20.0	203.6	4 697	51.9	53	2 719	57.9
23.7	253.3	6 566	77.0	53	4 033	61.4
26.9	299.7	8 631	103.2	52	5 385	62.4
10.3	51.3	996	2.0	104	212	21.3
18.7	101.0	2 476	12.2	105	1 273	51.4
25.9	150.7	4 619	27.8	105	2 909	62.9
33.7	200.4	7 384	50.6	105	5 307	71.9
40.3	250.0	10 695	77.0	105	8 033	75.1
19.9	52.9	1 542	2.4	210	512	33.2
35.2	101.0	4 190	12.9	210	2 697	64.4
49.3	150.7	7 812	28.9	210	6 037	77.3
63.2	198.8	12 642	51.3	209	10 693	84.6
28.9	49.7	2 087	2.0	315	639	30.6
52.5	101.0	5 748	13.3	315	4 176	72.7
38.9	51.3	2 593	1.8	419	737	28.4
67.6	99.4	6 605	11.3	420	4 718	71.4

TABLE VII. - LOCKED-ROTOR TORQUE

Average current, A	Ripple-free dc torque, N-m	Chopped dc torque, N-m
50	2.7	3.1
100	14.0	14.2
150	32.3	32.9
200	55.6	57.4
250	84.5	86.5
300	114.3	116.6

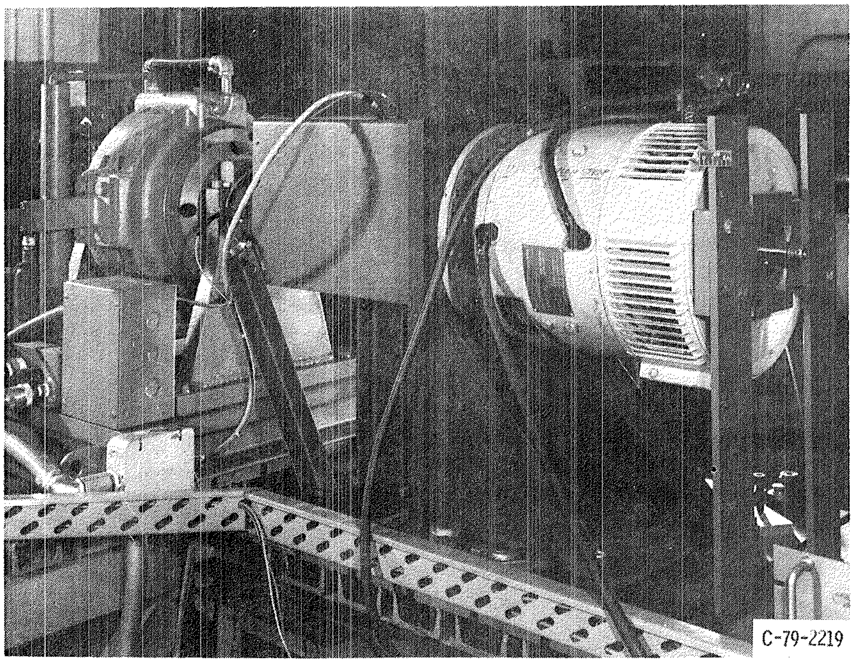

Figure 1. - Avon motor on test stand.

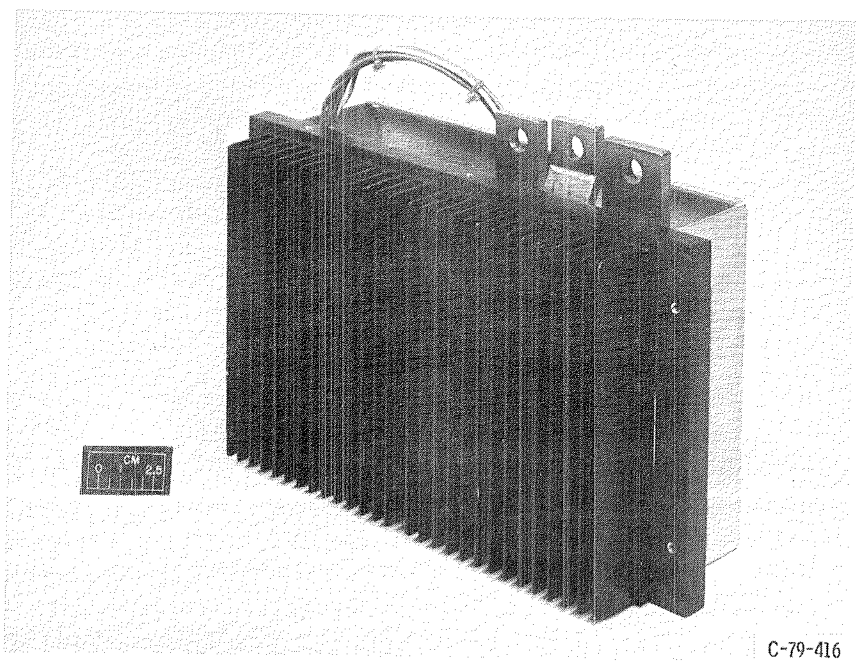

Figure 2. - EVC controller.

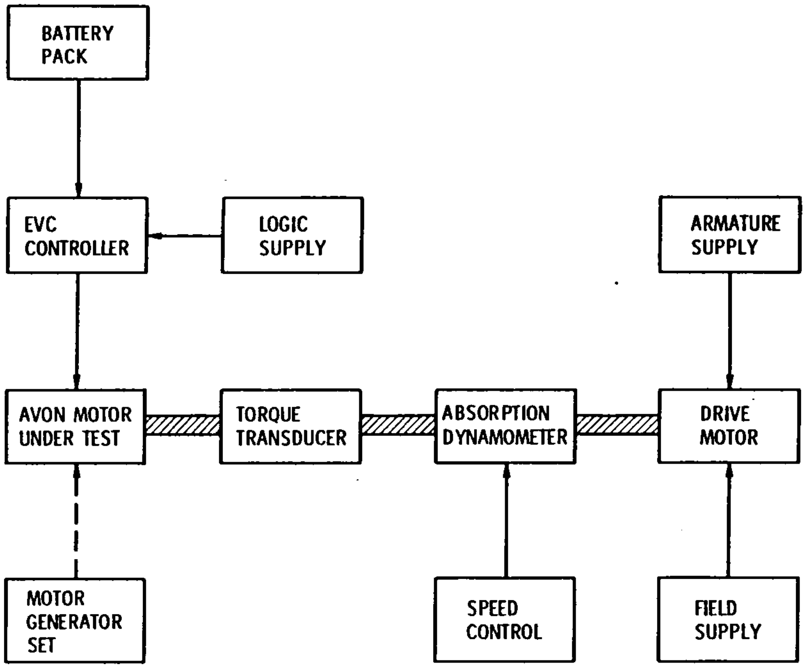

Figure 3. - Test apparatus.

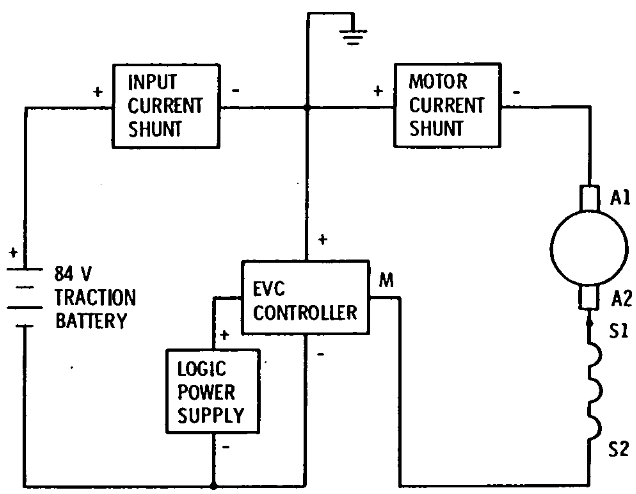

Figure 4. - Test electrical connection diagram.

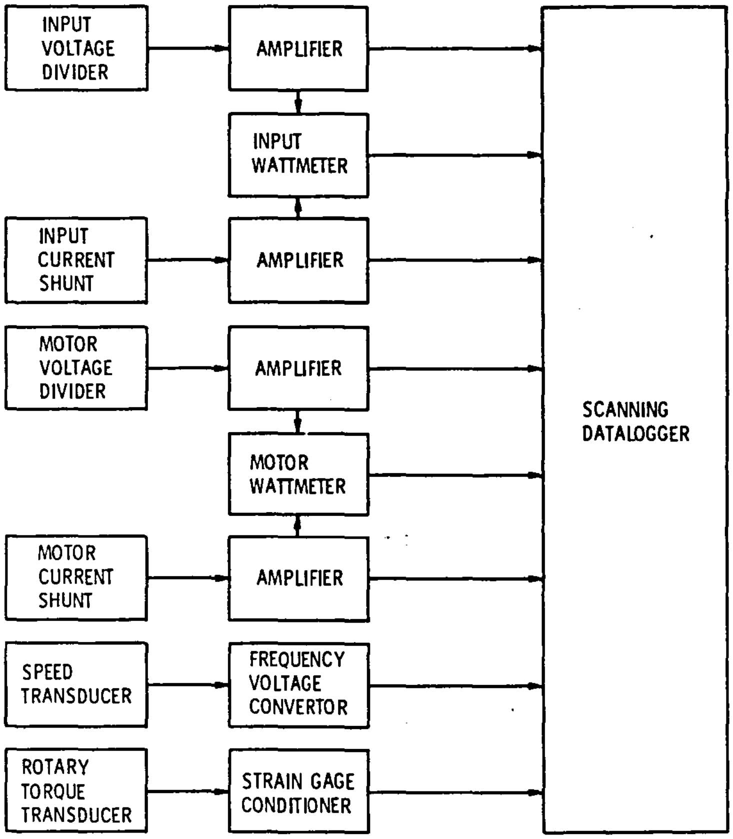

Figure 5. - Instrumentation system.

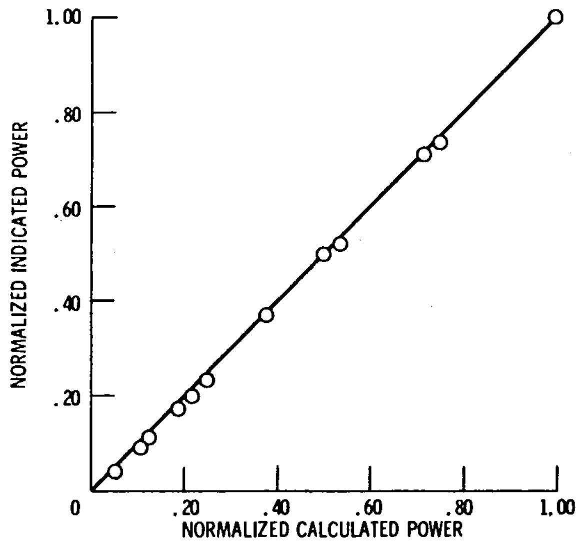

Figure 6. - Correlation of electronic wattmeter measurements with calculated power for ripple-free dc signals.

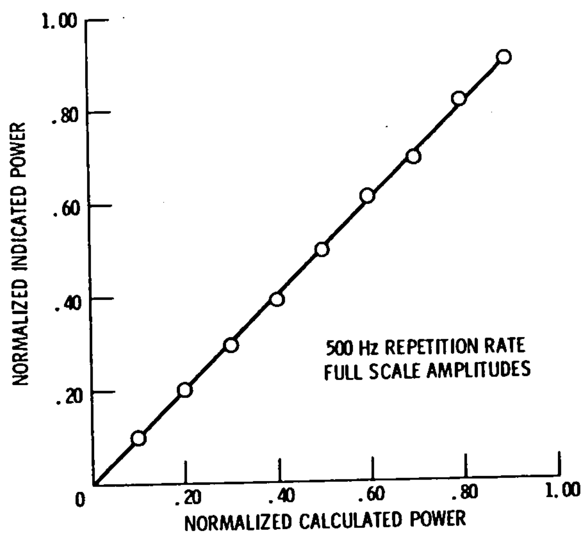

Figure 7. - Correlation of electronic wattmeter measurements with calculated power for rectangular pulse train signals of variable duty cycle.

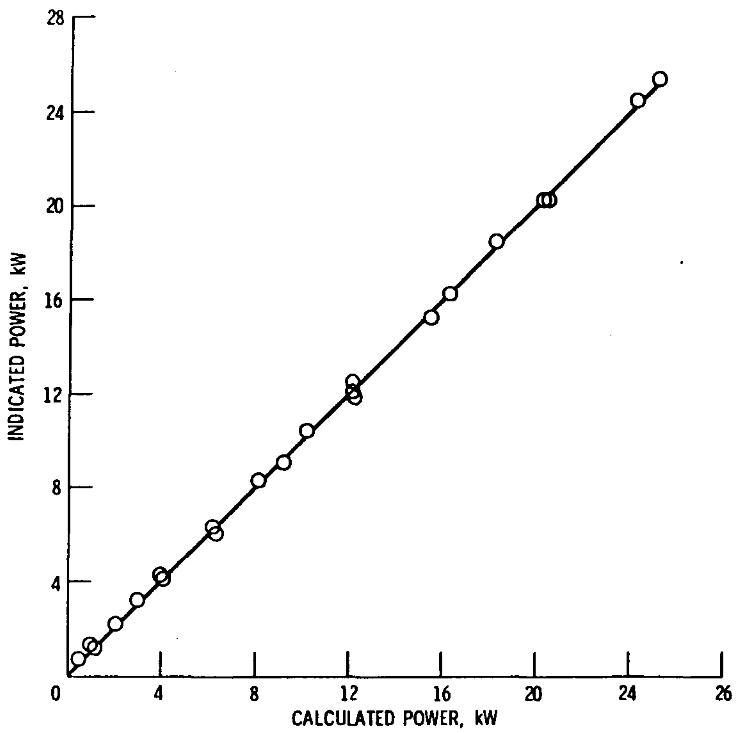

Figure 8. - Correlation of electronic wattmeter measurements with calculated power for ripple-free dc motor operation.

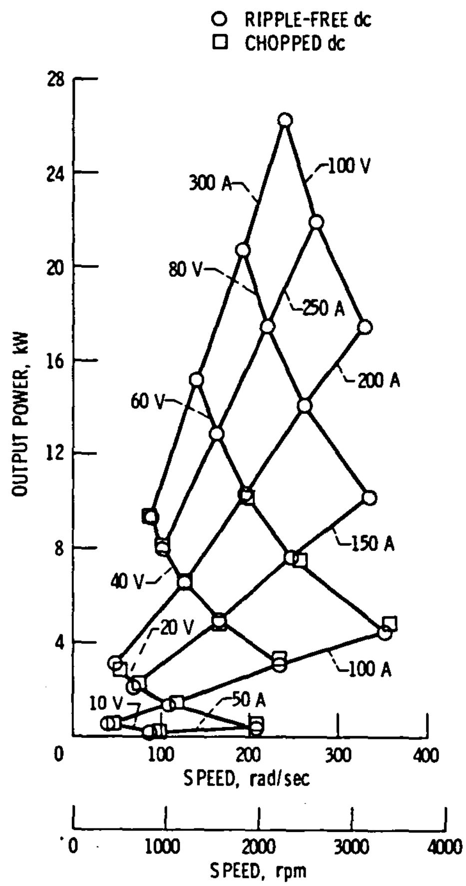

Figure 9. - Comparison of motor output power for ripple-free dc and chopped dc operation.

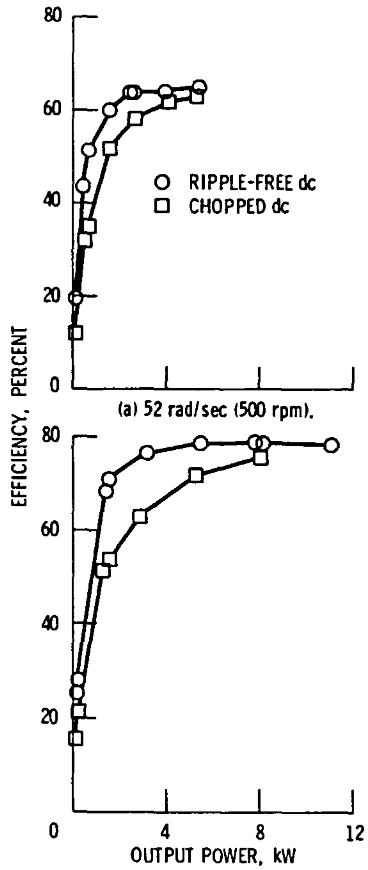

(b) 105 rad/sec (1000 rpm).

Figure 10. - Motor efficiency at constant speed.

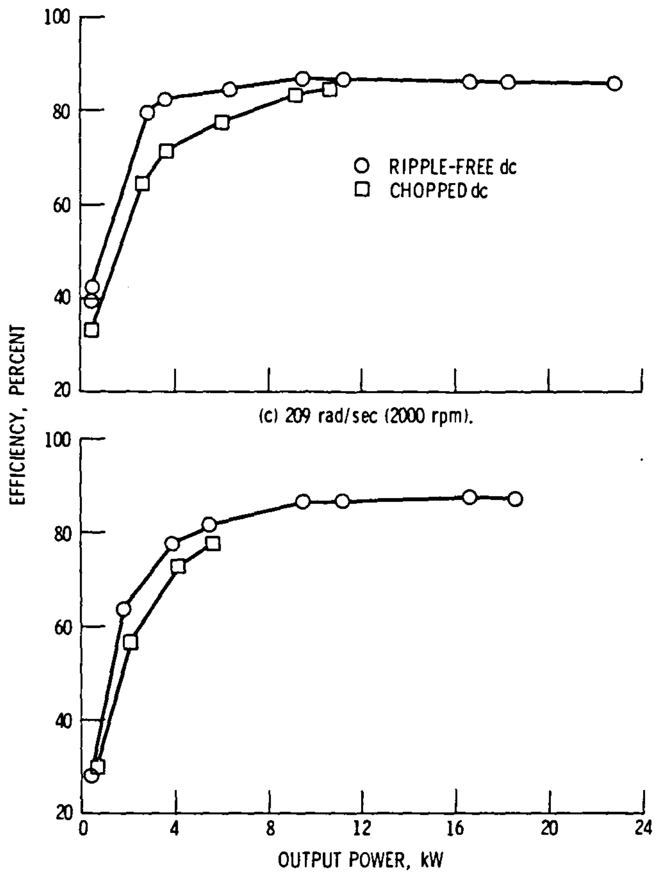

(c) 209 rad/sec (2000 rpm).

(d) 314 rad/sec (3000 rpm).

Figure 10. - Continued.

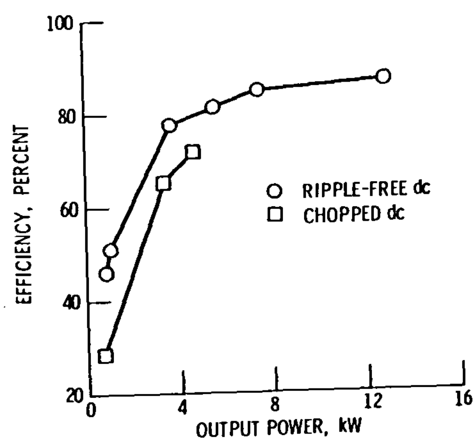

(e) 419 rad/sec (4000 rpm).

Figure 10. - Concluded.

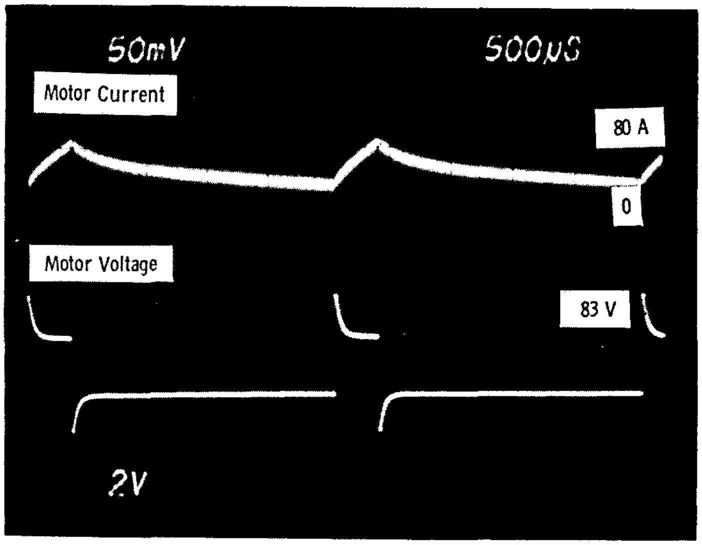

Average Current = 50A, Average Voltage = 10V.

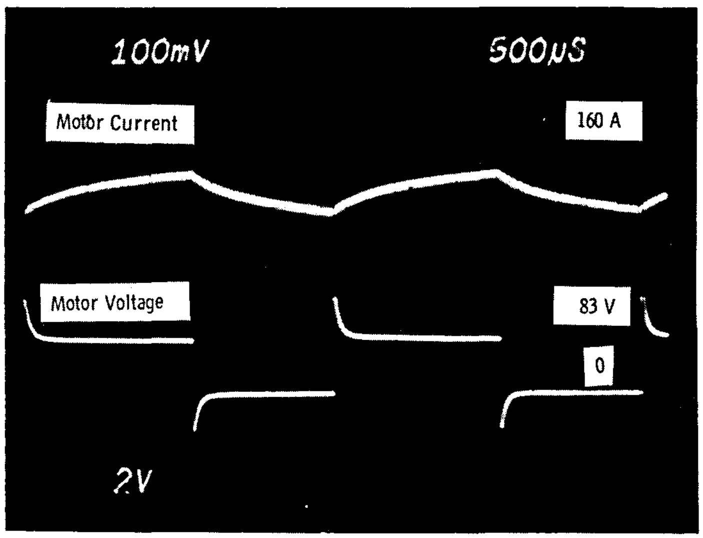

Average Current = 50A, Average Voltage = 40V.

Figure 11.- Typical motor voltage and current waveforms with pulse width modulated controller.

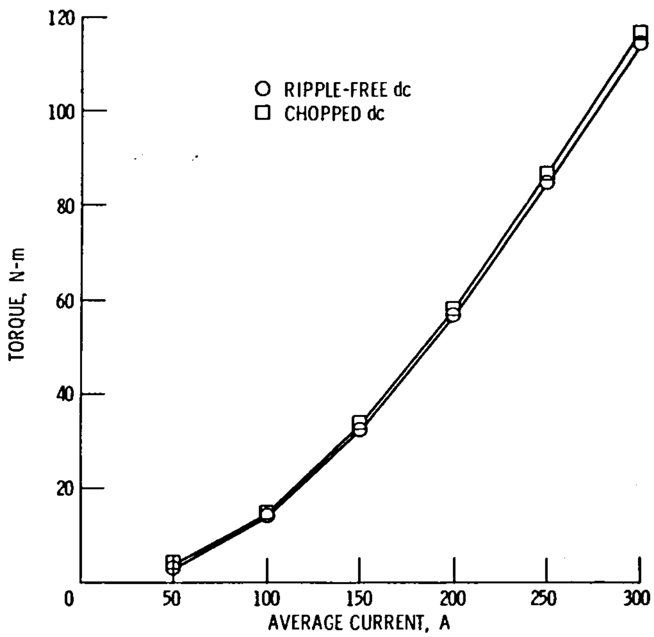

Figure 12. - Locked-rotor torque.

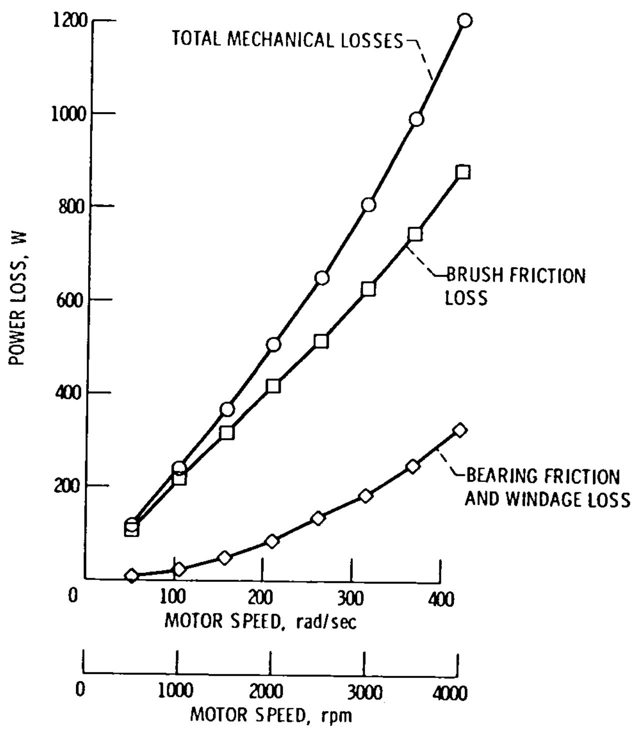

Figure 13. - Mechanical power losses.

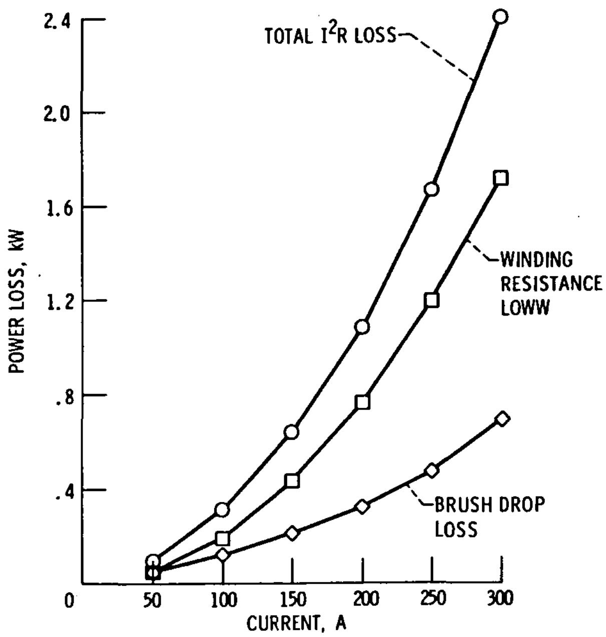

Figure 14. - I^2R power losses.

1. Report No.	2. Government Accession No.	3. Recipient's Catalog No.
NASA TM-79252		

4. Title and Subtitle

PERFORMANCE OF A 22.4-kW NONLAMINATED-FRAME dc SERIES MOTOR WITH CHOPPER CONTROLLER

5. Report Date

September 1979

6. Performing Organization Code

7. Author(s)

John R. Schwab

8. Performing Organization Report No.

E-163

9. Performing Organization Name and Address

National Aeronautics and Space Administration
Lewis Research Center
Cleveland, Ohio 44135

10. Work Unit No.

11. Contract or Grant No.

12. Sponsoring Agency Name and Address

U.S. Department of Energy
Transportation Energy Conservation Division
Washington, D.C. 20545

13. Type of Report and Period Covered

Technical Memorandum

14. Sponsoring Agency ~~Code~~ Report No.

DOE/NASA/1044-79/4

15. Supplementary Notes

Final report. Prepared under Interagency Agreement EC-77-A-31-1044.

16. Abstract

This report presents performance data obtained through experimental testing of a 22.4 kW (30 hp) traction motor using two types of excitation: ripple-free dc from a motor-generator set for baseline data and pulse-width modulated dc as supplied by a battery pack and chopper controller. For the same average values of input voltage and current, the motor power output was independent of the type of excitation. However, at the same speeds, the motor efficiency at low power output (corresponding to low duty cycle of the controller) was 5 to 10 percentage points lower on chopped dc than on ripple-free dc. The chopped dc locked-rotor torque was approximately 1 to 3 percent greater than the ripple-free dc torque for the same average current.

17. Key Words (Suggested by Author(s))

Electric vehicles
Electric motor

18. Distribution Statement

Unclassified - unlimited
STAR Category 33
DOE Category UC-96

19. Security Classif. (of this report)	20. Security Classif. (of this page)	21. No. of Pages	22. Price*
Unclassified	Unclassified		

* For sale by the National Technical Information Service, Springfield, Virginia 22161

End of Document